

Study of Combustion Characteristics of Ammonium Dinitramide/Polycaprolactone Propellants

Oleg P. Korobeinichev,* Alexander A. Paletsky,† Alexander G. Tereschenko,‡ and Evgeny N. Volkov§
Russian Academy of Sciences, 630090, Novosibirsk, Russia

This paper is devoted to the investigation of main characteristics and mechanism of combustion of the composite solid-rocket pseudopropellant based on ammonium dinitramide and polycaprolactone. Experimental data on the dependence of the burning rate on pressure in the pressure range of 4–8 MPa for ammonium dinitramide/polycaprolactone propellant with different additives and with polycaprolactone of different molecular weight are presented in the paper. The dependence of propellant burning rate on particle size of oxidizer and initial temperature has been also investigated. Composition of the combustion products of the propellant at pressures of 4 MPa using two different systems of sampling has been determined. The temperature profile in the combustion wave of some propellants has been obtained with aid of thin flat thermocouples. Temperature of the final combustion products of the propellant without additive and for some propellants with additive has been determined by a thermocouple method. Also the influence of a CuO catalyst on temperature profile has been investigated. Flame structure of ammonium dinitramide/polycaprolactone propellant at 0.1 MPa has been studied. Data obtained elucidating combustion mechanism and place of action of catalyst are discussed.

Nomenclature

A	=	factor in pressure dependence of the burning rate
C	=	coefficient of specific heat of condensed phase
C_p	=	coefficient of specific heat of gas phase at constant pressure
D_{mn}	=	mean size (diameter)
m	=	mass burning rate
P	=	pressure, MPa
Q	=	heat release in the reaction layer of the condensed phase
q	=	heat feedback from gas into condensed phase
q_m	=	heat of melting
r_b	=	burning rate, mm/s
T	=	temperature
T_s	=	burning surface temperature
T_0	=	initial propellant temperature, °C
β	=	temperature sensitivity, %/K
λ	=	coefficient of heat conductivity of gas phase
ν	=	pressure exponent
Φ	=	heat-release rate in the gas phase
ϕ	=	temperature gradient in gas phase close to the burning surface

Introduction

AMMONIUM dinitramide (ADN) is a powerful chlorine-free oxidizer, which can replace ammonium perchlorate (AP) in solid-rocket propellants. Because the combustion products of ADN-based propellants are not toxic, these propellants are environmentally friendly, and investigation of them is of great interest. An ADN-based propellant is a convenient system for investigation of the mechanism and chemistry of composite solid-rocket propellant

combustion because of the simplicity of the oxidizer. (ADN molecule contains only three elements: H, N, and O.) Important physicochemical properties and combustion characteristics of ADN and ADN-based propellants were published for the first time in Ref. 1. ADN has a higher heat of formation than AP, the common oxidizer of solid-rocket propellant; therefore, ADN-based propellants have higher specific impulse than AP-based propellants.^{1,2} The study of the combustion mechanism of pure ADN was the subject of several investigations.^{3–6} It was found that the burning rate of ADN is controlled by reactions in the condensed phase. A multizone flame structure was also established. At present, however, there are only a few papers that are devoted to the study of the combustion characteristics and combustion mechanism of composite ADN-based propellants and sandwiches with different types of binder such as hydroxyl-terminated polybutadiene (HTPB),^{7,8} glycidyl azide polymer,^{8,9} paraffin,^{3,10} poly(diethyleneglycol 4,8-dinitraza undecanate) (ORP-2A)/nitrate ester, (NE)¹¹ polycaprolactone polymer/NE,¹¹ and polybutadiene polymer.¹²

One of the objectives of the study of propellant combustion mechanism is the development of a combustion model that can predict combustion characteristics of solid propellants. The development of a combustion model describing composite solid propellant requires information on propellant flame structure. As a model of composite solid propellant, sandwiches based on oxidizer and binder are used. Flame structure of ADN-based sandwiches with various energetic and nonenergetic binders has been investigated in Ref. 13. Results showed either no or insignificant effects of diffusion flames on the processes controlling the propellant burning rate in the pressure range from 0.1 to 1.4 MPa. However, the burning rates of sandwiches such as ADN/(ADN/HTPB)/ADN and ADN/PBAN/ADN increased nearly 1.5-fold with the pressure increase from 1.5 to 7 MPa (data of Ed. Price, Georgia Tech. University, USA). This suggests a possible influence of the ADN-binder diffusion flames on the burning rate of sandwiches. It has been shown in Ref. 7 that the reactions in the condensed phase control ADN/HTPB propellant combustion.

The most important combustion characteristics of a rocket propellant in terms of practical application are specific impulse, burning rate r_b , parameter ν in dependence of the burning rate on pressure ($r_b = AP^\nu$), sensitivity of propellant burning rate to initial temperature, and composition and temperature of combustion products. It is not known at present what factor does determine the burning rate of ADN-based propellants. Combustion instability of pure ADN takes place in the pressure range of 2–10 MPa (Ref. 3). However, even

Received 29 March 2002; revision received 4 November 2002; accepted for publication 4 November 2002. Copyright © 2003 by the American Institute of Aeronautics and Astronautics, Inc. All rights reserved. Copies of this paper may be made for personal or internal use, on condition that the copier pay the \$10.00 per-copy fee to the Copyright Clearance Center, Inc., 222 Rosewood Drive, Danvers, MA 01923; include the code 0748-4658/03 \$10.00 in correspondence with the CCC.

*Professor, Head of Laboratory, Laboratory of Kinetics of Combustion Processes, Institute of Chemical Kinetics and Combustion; korobein@ns.kinetics.nsc.ru. Associate Fellow AIAA.

†Researcher, Institute of Chemical Kinetics and Combustion.

‡Researcher, Institute of Chemical Kinetics and Combustion.

§Engineer, Institute of Chemical Kinetics and Combustion.

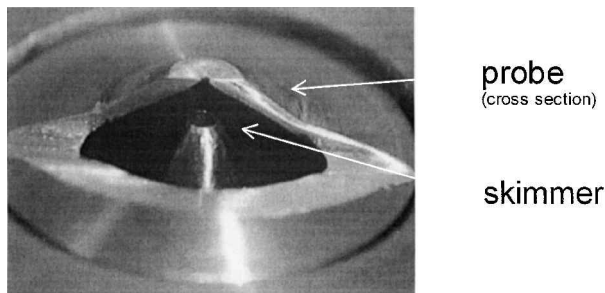


Fig. 2 Image of probe in cross section and skimmer.

skimmer is presented. Sampled gas flows through the skimmer in chamber 2 and then through the diaphragm with diameter of $40\ \mu\text{m}$ in chamber of mass-spectrometer's analyzer ($P \sim 2 \times 10^{-6}$ torr). The quantitative determination of CO and N_2 is one of the main problems of analysis of combustion products by time-of-flight mass spectrometer (TOFMS) because both of these gases contribute to the peak with mass 28. Two types of experiments were conducted. In the first one the combustion products directly entered the inlet system of TOFMS. In the second one a flow of oxygen was added to sampled combustion products in chamber 2 and resulting mixture passed through the layer of granules of CuO catalyst heated to a temperature around 870 K. In this case CO oxidized to CO_2 . Oxidation of CO allows us to get rid of its contribution to the peak with mass 28. The joint processing of data from both experiments makes the determination of concentrations of CO and N_2 in combustion products possible.

Probe mass spectrometry is the most effective and universal method for investigation of solid propellant flame structure.¹⁷ It allows the detection of all of the stable species present in the flame and also the ability to determine their concentrations and their spatial distributions. Flame structure has been studied at 0.1 MPa of argon using a setup¹⁸ with molecular beam sampling system combined with TOFMS. Calibrations⁵ were conducted for N_2 , O_2 , CO, CO_2 , N_2O , NH_3 , NO, HNO_3 , and H_2O . Calibration for water was conducted by vaporization of a drop of water in argon flow. Accuracy of measurement of species mole fractions in the range of 0.1–0.4 (H_2O , N_2 , N_2O , NO, and CO_2) was $\sim 10\%$. For species with mole fractions less than 0.1, the error was 20–30%. The temperature of the final combustion products was measured by Π -shaped WRe(5%)–WRe(20%) thermocouples with a shoulder length of ~ 3 mm, made of wire of $100\ \mu\text{m}$ in a diameter. The thermocouples were located at a distance of ~ 2 –5 mm from the strand surface. The error in determination of the temperature of the final combustion products was equal to ± 25 K. Temperature profiles in the propellant combustion wave at 4 MPa were measured by ribbon WRe(5%)–WRe(20%) thermocouples (thickness of 13–15 μm and width of ~ 140 –150 μm) embedded in the strand.

Results

Burning Rate

Influence of Polycaprolactone Molecular Weight

Data on the dependence of the burning rate r_b on pressure for $St_b(1250)$ and $St_b(10,000)$ propellants over a pressure range of 4–8 MPa are shown in Fig. 3. Parameters A and ν of the dependence of the burning rate on pressure $r_b = AP^\nu$ are given in Table 1. The $St_b(10,000)$ has a high pressure dependence exponent ($\nu = 1$). Replacement of PCL(10,000) in the propellant by a polymer with the same structure and chemical composition, but with lower molecular weight (1250) and lower melting point, led to the increase of the burning rate (by 1.5 times at 4 MPa and by 1.2 times at 8 MPa) and to the decrease of parameter ν to 0.7 (Fig. 3 and Table 1). The possible reason of observed difference in burning rate of these two propellants is considered in the discussion section.

Influence of Particle Size of ADN

It was shown that particle size of oxidizer influences the burning rate of $St_b(10,000)$. The parameter ν for propellant with bimodal

Table 1 Calculated specific impulse at 4 MPa and parameters of pressure dependence of the burning rate for St_b -based propellants at 4–8 MPa

Propellants	Specific impulse, s	$St_b(1250)$		$St_b(10,000)$	
		A	ν	A	ν
90% St_b + 10% Al	255.3	11.67	0.50	—	~ 1.0
90% St_b + 10% ALEX	255.3	6.16	0.71	—	—
88% St_b + 10% ALEX + 2% CuO	252.3	12.0	0.49	—	—
90% St_b + 10% RDX	249.3	—	—	9.63	0.54
90% St_b + 10% HMX	249.3	—	—	8.40	0.57
St_b	247.5	8.74	0.70	3.79	1.00
99% St_b + 1% CuO	245.7	12.29	0.55	7.29	0.69
98% St_b + 2% Pb_3O_4	244.7	12.92	0.42	6.22	0.64
98% St_b + 2% PbO	244.7	—	—	7.01	0.70
98% St_b + 2% PbO_2	244.7	—	—	5.41	0.82
98% St_b + 2% CuO	243.9	15.30	0.44	9.10	0.60
90% St_b + 10% AN	242.2	—	—	4.60	0.84
90% St_b + 10% AP	241.6	—	—	5.62	0.73

Table 2 Burning rate r_b at different initial temperatures T_0 °C

Propellant	P, MPa	T_0 , °C				
		−50	−20	+20	+30	+50
$St_b(1250)$	4	18.9	18.4	23	24.1	—
	8	31.1	31.3	37.5	39.1	—
$St_b(10,000)$	4	—	11.5	15.2	—	19.9
	8	21.9	21.9	30.3	—	29.6

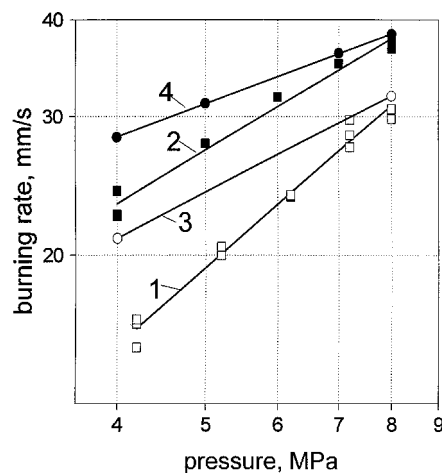


Fig. 3 Dependence of propellant burning rate on pressure: 1 (\square), $St_b(10,000)$; 2 (\blacksquare), $St_b(1250)$; 3 (\circ), 98% $St_b(10,000)$ + 2% CuO; and 4 (\bullet), 98% $St_b(1250)$ + 2% CuO.

oxidizer decreased to 0.72 in comparison with propellant on base of fine oxidizer ($\nu = 1.0$) within a pressure range of 3–8 MPa. Values of the burning rate for propellant with bimodal oxidizer are very close to propellant with fine oxidizer. However, for $St_b(10,000)$ propellant with fine oxidizer there are two regions with different parameter ν in the pressure range 2–8 MPa, whereas propellant with bimodal oxidizer has one parameter ν within a pressure range of 3–8 MPa (Fig. 4).

Influence of Initial Temperature

Burning-rate dependencies on the initial temperature T_0 , for $St_b(1250)$ and $St_b(10,000)$ propellants at pressures of 4 and 8 MPa are presented in Table 2. The minimum temperature studied for both propellants was -50°C , and the maximum ones were $+30^\circ\text{C}$ for $St_b(1250)$ and $+50^\circ\text{C}$ for $St_b(10,000)$. The maximum initial temperature did not exceed the melting point of the corresponding polymer. Temperature sensitivity of the propellants β was defined using the formula $\beta = d[\ln(r_b)]/dT$. Absolute error in the measurement of β was $\pm 0.15\%/K$. Temperature sensitivity of the burning

Table 3 Temperature sensitivity β over different temperature ranges

Propellant	P, MPa	Temperature range, °C			
		-50 to -20	-20 to +20	+20 to +30	+20 to +50
$St_b(1250)$	4	≤ 0.15	0.56	0.47	— ^a
	8	≤ 0.15	0.45	0.42	— ^a
$St_b(10,000)$	4	— ^a	0.69	— ^a	0.89
	8	≤ 0.15	0.81	— ^a	≤ 0.15

^aDid not measure in experiment.

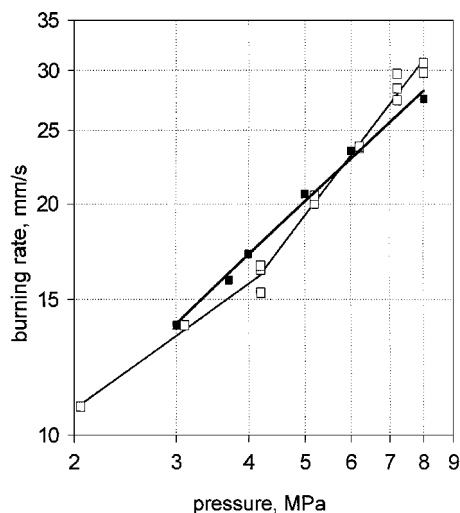


Fig. 4 Dependence of propellant burning rate on pressure: 1 (□), $St_b(10,000)$; and 2 (■), $St_b(10,000)$ with bimodal ADN.

rate over different temperature ranges at 4 and 8 MPa is presented in Table 3.

The decrease of the initial temperature from -20 – -50°C did not change the burning rate of the propellants under investigation at pressures of 4 and 8 MPa (Table 2). Besides, combustion instability took place at temperature of -50°C , that is, possibly these conditions are close to the combustion limit of the ADN/PCL composite propellant. In the temperature range of -20 – $+20^\circ\text{C}$ β for $St_b(10,000)$ is larger than β for $St_b(1250)$ and is equal to 0.7–0.8 and 0.5–0.6 %/K, respectively (Table 3). A further increase of temperature of $St_b(1250)$ to $+30^\circ\text{C}$ had little change on β at pressures of 4 and 8 MPa. With an increase of initial temperature of $St_b(10,000)$ propellant to $+50^\circ\text{C}$, β slightly increased to $\sim 0.9\%$ /K at 4 MPa pressure and decreased to practically zero at 8 MPa.

Influence of Different Additives on the Burning Rate

CuO and Cu₂O. Addition of 2%CuO to $St_b(1250)$ and $St_b(10,000)$ propellant increased the burning rate of these propellants at 4 MPa (Fig. 3) and practically had little effect on the burning rate at 8 MPa. Qualitatively, the effect of CuO on the burning rate of the propellant does not depend on the properties of the polycaprolactone used. Quantitatively, the effect of an additive on the burning rate is characterized by ratio of the burning rates of propellant with and without an additive. Addition of 2%CuO resulted in the increase of the burning rate of $St_b(1250)$ by a factor of 1.23 and of $St_b(10,000)$ by 1.38 at 4 MPa. At addition of 2% CuO parameter ν decreased by a factor of 1.6: to 0.44 for $St_b(1250)$ and to 0.60 for $St_b(10,000)$ (Table 1). Addition of 1%CuO resulted in effects similar to the addition of 2%CuO: an increase of the burning rate of St_b , but in a lesser degree. The burning rate of $St_b(1250)$ increased by 1.15 times and of $St_b(10,000)$ by 1.26 times at 4 MPa. Addition of both 1%CuO and 2%CuO did not change the burning rate of St_b at 8 MPa.

The main ingredient in the propellants under investigation is ADN (89.08%). Therefore, the effect of the addition of CuO on ADN burning rate has been explored. Combustion of pure ADN over the pressure range of 2–8 MPa is unstable.³ Our investigation confirmed this fact. However, addition of 2%CuO to pure ADN resulted in stabiliza-

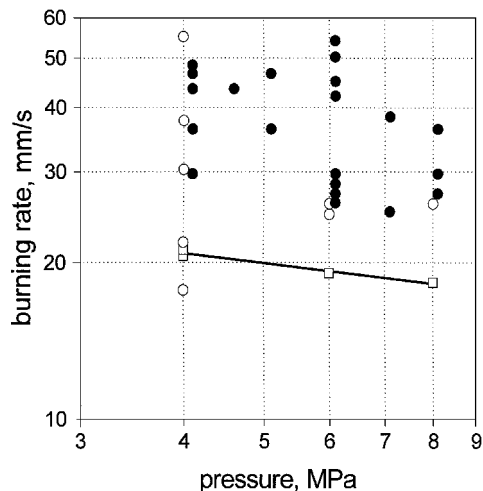


Fig. 5 Dependence of the burning rate of ADN + catalyst mixture on pressure: □, 98%ADN + 2%CuO; ○, ADN (our data); and ●, ADN (Ref. 3).

tion of ADN combustion. Burning rates of the 98%ADN + 2%CuO mixture at pressures of 4–8 MPa are compared with those for pure ADN in Fig. 5. The burning rates of 98%ADN + 2%CuO mixture are beneath the lower boundary of the observed scatter of the burning rates of pure ADN. The pressure exponent for 98%ADN + 2%CuO mixture in the pressure range of 4–8 MPa is negative [An effect similar to that attained by adding of Cu₂O (Ref. 4).], that is, the burning rate of this mixture decreases with the increase of pressure from 4 to 8 MPa. The different influence of CuO on the burning rate of pure ADN at 4–8 MPa and that of the St_b propellant might indicate a difference in the mechanism of action of CuO in these two cases.

Addition of 2%Cu₂O promoted combustion of $St_b(10,000)$ at pressure of 4 MPa and decreased parameter ν similar to addition of 1%CuO. During the pressing of the mixture of 98% $St_b(1250)$ with 2%Cu₂O, ignition and burning of this mixture took place; therefore, experiments with 98% $St_b(1250)$ + 2%Cu₂O propellant were not conducted.

PbO and PbO₂. Propellants with additive of PbO and PbO₂ have been also investigated. The effect of 2%PbO on the burning rate of $St_b(10,000)$ at an initial pressure of 4 MPa is less than the effect of 2%CuO. Addition of PbO to $St_b(1250)$ in the amounts of 1 and 2% resulted in nonsteady combustion at the initial pressure of 4 MPa. The burning rate at this pressure varied ~ 2 times during the combustion of one strand. Addition of 2%PbO₂ to $St_b(10,000)$ did not particularly influence the pressure dependence of the burning rate (Table 1).

Pb₃O₄. As it is shown in Fig. 6, a decrease in the burning rate of both baseline propellants took place at an initial pressure of 8 MPa upon addition of 2%Pb₃O₄. When the initial pressure was decreased from 8 to 4 MPa, the influence of Pb₃O₄ on the burning rate decreased. Addition of a mixed catalyst, 2%Pb₃O₄ + 2%CuO, did not result in the expected combined effect of the individual catalysts: increase of the burning rate at 4 MPa (CuO) and decrease of the burning rate at 8 MPa (Pb₃O₄). The effect of this composite additive turned out to be very close to that of 2%CuO. In this case Pb₃O₄ played a passive role, at best.

Other Oxidizers and Cyclic Nitramines. The effect of different additives in the amount of 10% to $St_b(10,000)$ propellant has been studied. In Table 1 the parameters of the dependence of the burning rate on pressure over a pressure range of 4–8 MPa for propellants based on $St_b(10,000)$ are shown.

Addition of 10% AN or 10% AP to $St_b(10,000)$ resulted in a decrease of the burning rate at a pressure of 8 MPa and had almost no effect at 4 MPa and parameter ν decreased to 0.84 (AN) and

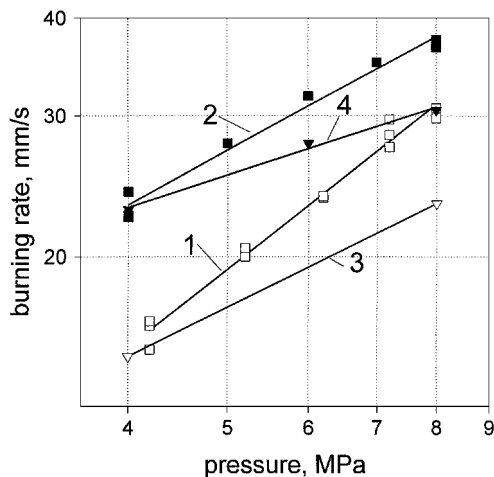


Fig. 6 Dependence of propellant burning rate on pressure: 1 (\square), $St_b(10,000)$; 2 (\blacksquare), $St_b(1250)$; 3 (∇), 98% $St_b(10,000)$ + 2% Pb_3O_4 ; and 4 (\blacktriangledown), 98% $St_b(1250)$ + 2% Pb_3O_4 .

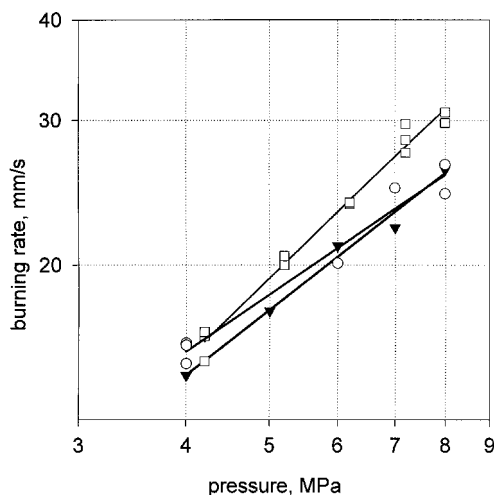


Fig. 7 Dependence of propellant burning rate on pressure: \square , $St_b(10,000)$; \blacktriangledown , 90% $St_b(10,000)$ + 10% AN; and \circ , 90% $St_b(10,000)$ + 10% AP.

0.73(AP) (Fig. 7). Addition of 10% RDX or 10% HMX led to an increase of the burning rate at 4 MPa pressure and did not effect the burning rate at 8 MPa. Addition of cyclic nitramines decreased v to 0.57 (HMX) and 0.54 (RDX) (Fig. 8). Propellants with additives of AN and AP have a positive oxygen balance, and propellants with additives of RDX or HMX have a negative one.

Aluminum. Addition of 10% Al to $St_b(10,000)$ did not change parameter v , but resulted in worse scatter of the data on the burning rate (Fig. 9). Parameters of the dependence of the burning rate of $St_b(1250)$ propellant with additives of 10% Al (or ALEX) and 10% ALEX + 2% CuO are presented in Table 1.

As it shown in Fig. 9, addition of fine aluminum slightly decreased the burning rate of the propellant at 8 MPa and did not affect it at 4 MPa. At the same time addition of ALEX in the same amount (10%) to $St_b(1250)$ propellant strongly decreased the burning rate over the pressure range of 4–8 MPa and did not change parameter v . Use of ultrafine aluminum (ALEX) in propellants is necessary to achieve more complete oxidation and the concomitant increase in specific impulse. Subsequent addition of 2% CuO resulted in a significant increase of the burning rate up to that of the propellant with 10% Al additive. Simultaneous addition of ALEX and CuO to the propellant might allow one to reach the optimal characteristics of the propellant (high burning rate, high calculated specific impulse, low v).

Table 4 Temperature of the final combustion products of $St_b(10,000)$ -based propellants at 4 MPa

Propellant	T_{calc} , K	T_{exp} , K	ΔT , K
St_b	2960	2870	90
98% St_b + 2% PbO_2	2950	2915	35
98% St_b + 2% Pb_3O_4	2950	2910	40
90% St_b + 10% AN	2873	2785	88
90% St_b + 10% AP	2909	2870	39

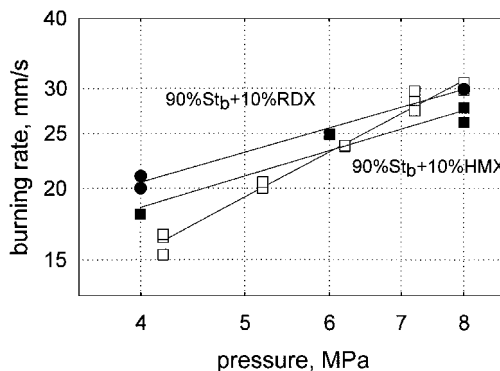


Fig. 8 Dependence of propellant burning rate on pressure: \square , $St_b(10,000)$; \blacksquare , 90% $St_b(10,000)$ + 10% HMX; and \bullet , 90% $St_b(10,000)$ + 10% RDX.

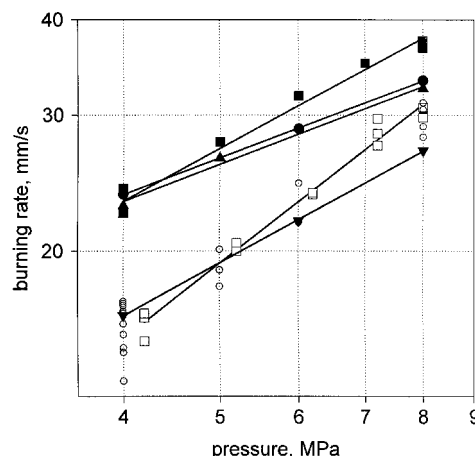


Fig. 9 Dependence of propellant burning rate on pressure: \square , $St_b(10,000)$; \circ , 90% $St_b(10,000)$ + 10% Al; \blacksquare , $St_b(1250)$; \blacktriangledown , 90% $St_b(1250)$ + 10% ALEX; \bullet , 88% $St_b(1250)$ + 10% ALEX + 2% CuO; and \blacktriangle , 90% $St_b(1250)$ + 10% Al.

Results of Calculations of Specific Impulse

Specific impulse for base propellant (St_b) and also for propellant with additives at 4 MPa and exit pressure of 0.1 MPa was calculated using code "Astra."¹⁹ Results of calculations are presented in Table 1. Addition of such energetic additives as aluminum and nitramines (RDX, HMX) to St_b increases specific impulse. Addition of lead and copper oxides and also oxidizers with less enthalpy of formation (AP, AN) results in a decrease of specific impulse. Combination of two additives (10% ALEX and 2% CuO) gives both a high specific impulse and a low parameter v .

Specific impulse for AP/PCL propellant of stoichiometric composition was also calculated.¹⁹ The specific impulse of this propellant is less than that of ADN/PCL by 12.9 s and is equal to 234.6 s.

Temperature and Composition of Final Combustion Products

In Table 4 experimental values for the temperature T_{exp} of the final combustion products of $St_b(10,000)$ propellant with and without additives at 4 MPa are presented in comparison with the calculated thermodynamic equilibrium values ($\Delta T = T_{calc} - T_{exp}$). The thermodynamic equilibrium composition of the combustion products and temperatures T_{calc} were calculated with the computer code "Astra."¹⁹ We could not measure the temperature of the final

Table 5 Temperature and concentrations of the final combustion products (percents by volume) of $St_b(10,000)$ and $90\%St_b(10,000) + 10\%Al$ propellant at 4 MPa

Propellant	T, K	H ₂ O	N ₂	CO ₂	CO	O ₂	NO	H ₂	OH	H	O
St_b , calc ¹⁹	2960	43.7	34.8	10.5	3.6	1.8	0.9	2.0	2.2	0.2	0.3
St_b , exp ^a	2870	48	35.8	10.9	1.3	1.7	0.6	1.1	— ^b	— ^b	— ^b
$90\%St_b + 10\%Al$, calc ¹⁹	3392	34.5	34.4	4.4	9.5	0.8	0.9	9.0	3.6	2.2	0.5
$90\%St_b + 10\%Al$, exp ^a	— ^b	41.0	37.0	6.7	6.7	1.4	0.5	6.2	— ^b	— ^b	— ^b

^aOne-stage sampling with following GC analysis. ^b— was not measured in experiment.

Table 6 Results of processing of temperature profiles in combustion wave of ADN/PCL propellant without and with 2% CuO and of ADN

Propellant	P, MPa	φ , K/m	m , kg/m ² s	q , J/kg	Q , J/kg	Φ , J/m ³ s
St_b	4	1.9×10^7	25.3	3.2×10^4	5.4×10^5	6.7×10^{11}
$98\%St_b + 2\%CuO$	4	1.3×10^7	36.3	1.6×10^4	6.3×10^5	6.6×10^{11}
Pure ADN ⁶	2	10^7	46.4	1.3×10^4	5.5×10^5	—

combustion products for propellants with additives of CuO and Al using uncovered thermocouples. Corrected data for heat loss by radiation²⁰ are presented in Table 4. In the case of $St_b(10,000)$ propellant at 4 MPa, this radiation correction for cylindrical thermocouples with a diameter of 0.1 mm was equal to ~ 190 K. Temperature of the final combustion products of $St_b(10,000)$ propellant with radiation correction measured by different thermocouples was equal to 2870 ± 25 K. This temperature is slightly less than the calculated equilibrium temperature [2960 K (Ref. 19)]. The increase of the initial pressure to 8 MPa did not change the temperature of the final combustion products of $St_b(10,000)$.

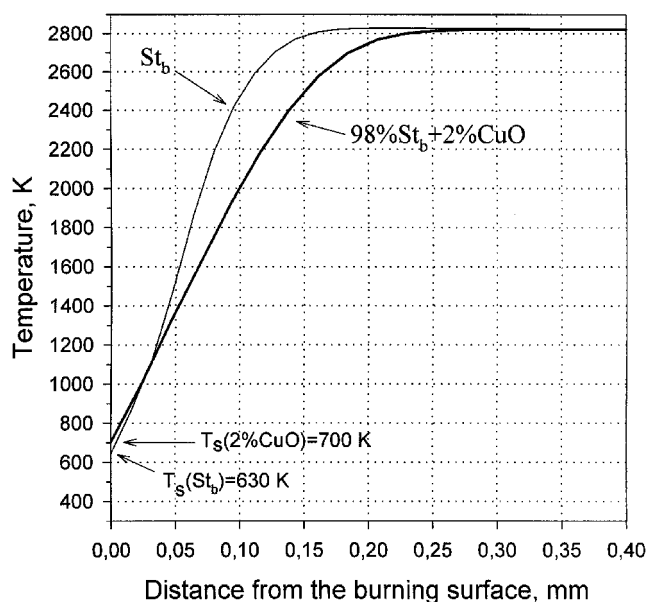
Final combustion temperatures for the baseline propellant and propellant with AN added are lower than the corresponding calculated thermodynamic equilibrium temperatures by ~ 90 K. In the case of the additives of AP and lead oxides, experimental and calculated temperatures are consistent with each other (within experimental error). Small additives of PbO₂ and Pb₃O₄ increased experimental temperature value for the baseline propellant by 35 and 40 K, respectively.

Application of the one-stage sampling system with subsequent gas chromatographic (GC) analysis of the composition of the combustion products of $St_b(10,000)$ allowed quantitative determination of such products as N₂, H₂, NO, O₂, CO, and CO₂ (Table 5). With the exception of NO, these combustion products are environmentally friendly. However, the concentration of NO in the combustion products at 4 MPa is less than 1%. Moreover, calculations showed that its concentration decreases to $\sim 0.02\%$ at the nozzle exit at 0.1 MPa (Ref. 19). The largest difference between experimentally determined and calculated equilibrium compositions of combustion products involves the concentration of CO. For more precise determination of the amount of CO in combustion products, a two-stage sampling system was used. Application of this system allowed the determination of the ratio between CO and CO₂ and thus a more precise value of CO concentration, which appeared to be $3.1 \pm 0.6\%$.

In Table 5 experimental and calculated¹⁹ compositions of the combustion products of $90\%St_b(10,000) + 10\%Al$ propellant at 4 MPa are presented. We could not measure concentration of H₂O; therefore, the content of H₂O in the combustion products was calculated with aid of material balance equations using the ratio of elements H:N:O:C in the initial propellant. Permanganometric method of analysis of the condensed combustion products²¹ showed that $\sim 93\%$ of the initial Al oxidized to Al₂O₃. This fact was taken into account in calculations of the composition of gaseous combustion products of aluminized propellant. According to the thermodynamic calculation, $\sim 99\%$ of the initial amount of aluminum oxidizes to Al₂O₃.

Thermal Structure of Propellant Combustion; Wave Place of Action of CuO Catalyst

To take into account the time response of the thermocouple in the flame when processing experimental data, we used the procedure proposed by Zenin.²² Corrected temperature profiles for

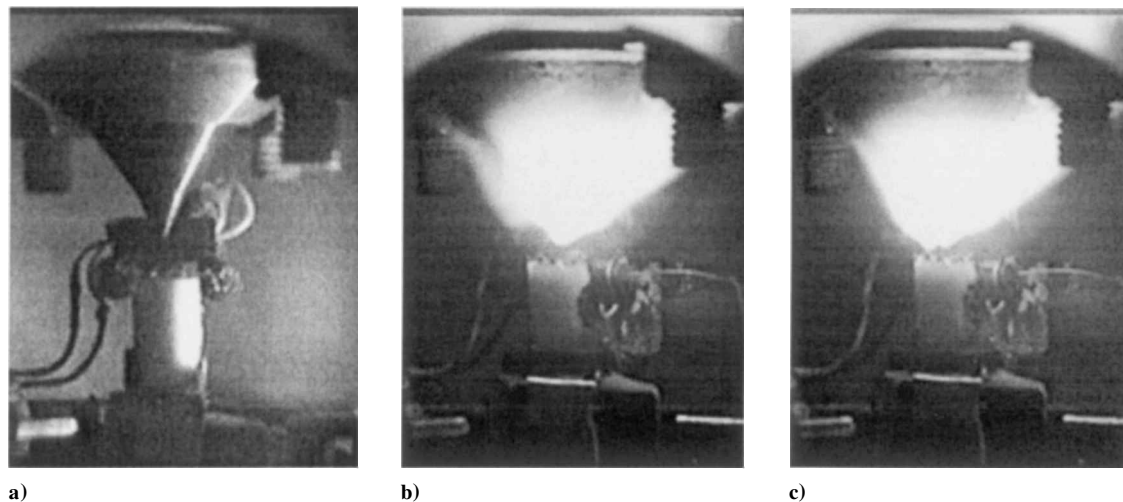
**Fig. 10** Corrected temperature profiles in combustion wave of $St_b(10,000)$ and $98\%St_b(10,000) + 2\%CuO$ propellants at 4 MPa.

$St_b(10,000)$ and $98\%St_b(10,000) + 2\%CuO$ at 4 MPa are shown in Fig. 10. Temperature of the propellant burning surface was determined by a method of "slope break" on the temperature profile²² in several experiments. Mean value of burning surface temperature T_s of $St_b(10,000)$ at 4 MPa was equal to 630 ± 10 K. It is close to the estimation of T_s for pure ADN (640 K) at 4 MPa (Ref. 6). The thickness of the thermal layer in the condensed phase (CP) was $\sim 180 \mu\text{m}$, and L width of the reaction zone in the flame of $St_b(10,000)$ was $\sim 150 \mu\text{m}$. The temperature gradient near the burning surface φ was $\sim 1.9 \times 10^7$ K/m. The addition of 2%CuO to St_b resulted in the increase of T_s by 70 K (Fig. 10) and the increase of L by 50 μm at 4 MPa.

Heat feedback q from the flame into the CP by heat conductivity was calculated by the equation $q = -\lambda(T)\varphi/m$, where $\lambda = 4.2 \times 10^{-2}$ W/m K. Heat release in the reaction layer of the CP was calculated using the formula $Q = C(T_s - T_0) - q + q_m$, where $C = 1.26 \times 10^3$ J/kg K, $q_m = 1.34 \times 10^5$ J/kg, $T_0 = 293$ K. The values of λ , C , q_m were the same as in the case of pure ADN.⁶ Heat-release rate in the flame was calculated by the approximate formula $\Phi = C_p \varphi m$, where $C_p = 1.39 \times 10^3$ J/kg K (Ref. 6). Addition of 2%CuO to St_b did not change Φ , but decreased q and increased Q by a value of 9.2×10^4 J/kg (Table 6). As a result, the burning rate increased. The data obtained indicate that reactions in the CP control the burning rate of ADN-based propellant. Accuracy of data presented in Table 6 is equal to $\pm 10\%$ for φ , $\pm 15\%$ for q , $\pm 5\%$ for Q , $\pm 5\%$ for m , and $\pm 15\%$ for Φ . Data obtained show that the place of action of the CuO catalyst is in the CP.

Table 7 Concentrations (in mole fractions) of species and temperature in flame of propellant $St_b(1250)$ at 0.1 MPa and of ADN at 0.6 MPa

Flame zone	T , K	H_2O	N_2	N_2O	NO	NH_3	HNO_3	H_2	CO	CO_2	O_2
Luminous zone (exp)	~2600	0.39	0.32	0	0.10	0	0	0.03	0.02	0.12	0.02
Thermodynamic calc. ¹⁹	2695	0.40	0.34	0	0.01	0	0	0.03	0.05	0.09	0.03
Dark zone (exp)	~1120	0.32	0.11	0.20	0.20	0.04	0.01	0.01	0.02	0.08	0.01
Pure ADN dark zone at $L_1 \sim 4$ mm (0.6 MPa) (Ref. 5)	~920	0.31	0.10	0.28	0.23	0.07	0.02	—	—	—	—

**Fig. 11** Video images of combustion of propellant $St_b(1250)$ at 0.1 MPa: a) before the experiment and b) and c) in different times during combustion ($\Delta t = 0.04$ s).

Flame Structure of $St_b(1250)$ Propellant at 0.1 MPa

Experiments showed that $St_b(10,000)$ propellant burned without a visible flame at 0.1 MPa. Brown residue (apparently, undecomposed polycaprolactone) remained on the strand holder after the experiment. Temperature of combustion products was ~ 670 K, which is close to that of pure ADN at 0.1 MPa (Ref. 5). So, one can suppose that at 0.1 MPa only the ADN burns, whereas PCL(10,000) only melts and partially decomposes. Replacement of PCL(10,000) by PCL(1250) resulted in the appearance of a visible flame. However, the flame did not cover the entire burning surface of the strand. Separate jets of flame moving over the strand burning surface during the combustion were observed (Fig. 11). So, the combustion of $St_b(1250)$ at 0.1 MPa has a torch character with formation of separate seats of burning on the burning surface. Video recording of the burning surface with 16-fold magnification revealed the processes that take place on the propellant surface during combustion. The following processes should be noted (see Fig. 12): 1) appearance of sites of darkening on the burning surface (a) with consequent transition of them in small dark spots (b); 2) fusion of these small spots into large spots (c, d), with arrows showing the direction of fusion; 3) appearance of two torches over large spots, the diameter of which is ~ 1 mm (e); and 4) one of torches lifts-off (f). These spots are probably drops of liquid undecomposed PCL on the molten surface of the ADN. Fusion of small drops of PCL in the bigger drops is caused by the lower melting point of PCL in comparison with ADN.

The measurement of temperature and the determination of combustion product composition were conducted in different experiments. The probe (or thermocouple) during the combustion was located either in the luminous zone (torch) or in dark zone (between torches or far from them). Analysis of the videotape recording allowed the determination of the flame zone, where the probe or thermocouple was located at the moment of measurement.

Results of two experiments on measurement of the temperature profile in flame of $St_b(1250)$ at 0.1 MPa, which confirm the conclusion regarding torch combustion of this propellant, are presented in Fig. 13. Curve 1 in Fig. 13 corresponds to the case when thermocouple was in the torch, and curve 2 corresponds to the case when it was between the torches. The videotape recording showed that a dark zone exists near the burning surface. The width of the dark zone

varies from ~ 1 mm (near bottom of torch) to 3–4 mm (region between torches). Thermocouple measurements revealed the existence of three zones in the flame (Fig. 13): 1) the narrow dark zone adjacent to the burning surface (width of the zone ~ 0.2 – 0.3 mm), where the temperature rose from ~ 600 to ~ 1200 K; 2) the dark zone (width of the zone ~ 0.5 – 3 mm), where the temperature slightly increased from 1200 to 1450 K; and 3) the luminous zone (torch), where the temperature increased to 2600 K at the distance of 4–8 mm.

Compositions of the combustion products in the luminous and dark flame zones of $St_b(1250)$ propellant are presented in Table 7. Temperature of the combustion products in the luminous zone, which is equal to 2600 K, is slightly less than the calculated equilibrium temperature [2695 K (Ref. 19)], that is, 100% completeness of combustion is not achieved. The presence of NO in combustion products confirms this conclusion. The elemental balance in the luminous zone was in satisfactory agreement ($\pm 5\%$) with that in the propellant. The calculated deficiency of carbon in the combustion products determined in the dark zone is equal to $\sim 50\%$ of the initial amount. This fact indicates that identification of carbon-containing products in the dark zone was incomplete. In addition, we have obtained peaks of the following unidentified masses in the mass spectrum of species near the burning surface of the $St_b(1250)$ propellant: 55, 57, 60, 67, 69, 70, 71, 73, 79, 81, 95, 108, 115. We suggest that masses from 55 to 115 correspond to the decomposition products of PCL.

Discussion

Analysis of Table 1 shows that by using different additives we can influence the specific impulse and burning rate of St_b propellant. Using additives of 2% CuO and 2% Pb_3O_4 parameter v can be significantly reduced, but at the same time specific impulse also decreases. Addition of nitramines in amount of 10% decreases parameter v and slightly increases specific impulse. To achieve propellants with high specific impulse and low parameter v , addition of 10% ALEX + 2% CuO can be done.

Temperature sensitivity of pure ADN over the pressure range of 4–6 MPa and temperature range of -50 – 20°C is lower than that for ADN/PCL propellant and is equal to 0.3–0.4%/K. But temperature sensitivity of pure ADN over the range of $+20$ – 80°C is larger than

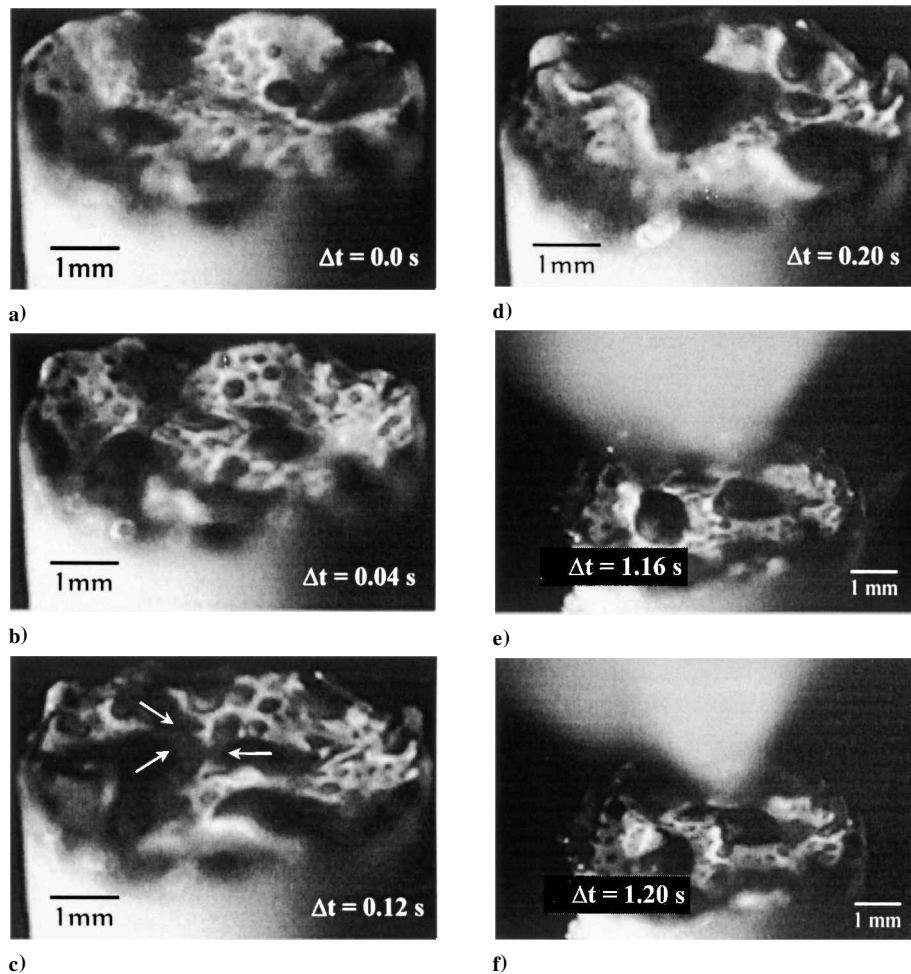


Fig. 12 Video images of the burning surface of propellant $St_b(1250)$ at 0.1 MPa obtained at 16-fold magnification.

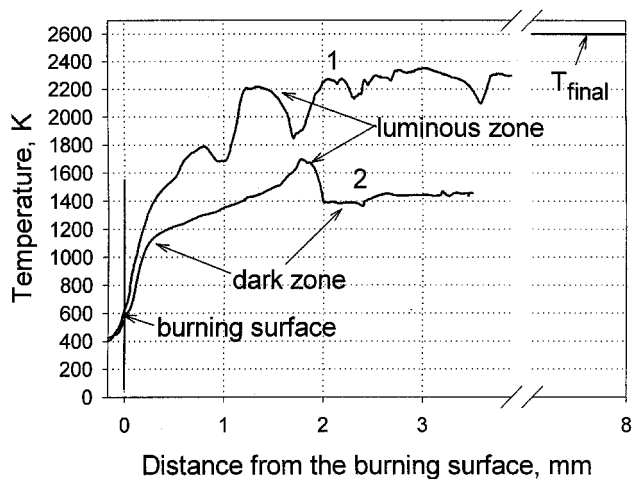


Fig. 13 Temperature profiles in flame of propellant ADN/PCL(1250) at 0.1 MPa.

for the ADN/PCL propellant and is equal to 1.5–1.6%/K (Ref. 6). So, although ADN is the main ingredient in the model St_b propellant, there is no correlation between temperature sensitivity for neat ADN and the ADN-based composite propellant.

Processing of the temperature profiles of both propellants [$St_b(10,000)$ with and without CuO] at 4 MPa showed that heat feedback from flame into CP is small in comparison with Q . Addition of CuO to the $St_b(10,000)$ increased Q , so that the place of action of CuO catalyst is CP. Therefore the reactions in the CP control combustion of the composite propellant as well as in the case of pure ADN.

The burning rate of the composite propellant is lower than that of pure ADN. As it was shown earlier,⁴ even small amounts ($\sim 1\%$) of organic fuel (plasticizer, rubber) significantly decrease the burning rate of pure ADN, which is contrary to the influence of additives of binder on the burning rate of AP. Addition of fuel probably inhibits the reactions of ADN decomposition in the CP likely depends on these properties. The rate of pyrolysis of PCL(1250) is significantly higher than that of PCL(10,000). Experiments on combustion of St_b propellants at 0.1 MPa just described confirm this conclusion. The difference between the rate of pyrolysis of PCL(10,000) and PCL(1250) could be the reason for their different influence on the burning rate of the propellant. Slower pyrolysis of PCL(10,000) leads to more accumulation of it on the burning surface. As a result of this, reactions of decomposition of ADN become significantly slower in the case of $St_b(10,000)$ propellant. The effect of inhibition of ADN decomposition in the condensed phase by minor additives of hydrocarbon fuels was discussed earlier in Ref. 4. The addition of fuel in the amount of only 1% resulted in a significant decrease of the burning rate of ADN at 0.1 MPa. The subsequent increase in fuel content up to 5% did not affect the burning rate much more. Such a behavior can be explained only assuming that fuel inhibits ADN decomposition. Thus, it is unlikely that the decrease of the burning rate of ADN upon the addition of hydrocarbon fuel can be explained solely by heat loss from evaporation/decomposition of the fuel. A paper devoted to the investigation of ADN/HTPB propellants⁷ provides additional confirmation of the prevalence of inhibition over the thermal effect. ADN/HTPB propellants with content of a HTPB in the amount of 3 and 7% had almost the same burning rates at 0.6 MPa (~ 7.3 and ~ 7.5 mm/s, respectively), which is

less than the burning rate of pure ADN by a factor of three at this pressure.

Initially, fuel (PCL) and oxidizer (ADN) are distributed uniformly in propellant mixture. During the combustion of $St_b(1250)$ at 0.1 MPa, redistribution of fuel on the burning surface, which is caused by formation of carbon-containing drops (Fig. 12), takes place. It results in variation of oxidizer/fuel ratio in the gas phase near the burning surface. One can assume that space near a small drop is filled mainly by products of decomposition of the oxidizer. The deficiency of carbon-containing products in dark zone confirms this statement. Thus, an invisible lean diffusion flame (dark zone in Table 7) with low product temperature occurs near the small drops of fuel. Fusion of several small drops of partially decomposed PCL into a larger one takes place on the burning surface (Fig. 12c) during the combustion. An intense flow of products from gasification and/or decomposition of fuel exists over the large drop. An interaction between the products of the decomposition of the oxidizer with the fuel decomposition products resulted in the appearance of a luminous diffusion flame directly over the drop. Lifetime of the drop (after appearance of the torch) is equal ~ 0.1 s. The presence of this luminous torch with high temperature of combustion products over the drop leads to an increase in heat feedback from gas phase to the burning surface and an increase in the temperature of the drop. As a result, an increase in the decomposition rate of the drop occurs. Volume and thickness of the drop then decrease during the combustion. The shape of the drop changes from near hemispherical to a more flat form. Then, some drops divide into smaller drops under the influence of the flow of oxidizer decomposition products from under the drop, and the torch disappears or moves over the remaining part of the drop.

It was discussed earlier that ADN at 0.1 MPa burns without flame (temperature of combustion products ~ 620 K) and that the combustion products of pure ADN contain ADN vapor.⁵ During the investigation of the flame structure of $St_b(1250)$ at 0.1 MPa peaks with 17, 30, 44, and 46 m/z were detected near the burning surface at temperature of ~ 600 K. The ratio between them is not given here, but this ratio corresponds to the ratio of these peaks in the mass spectrum of ADN vapor.⁵ The comparison of combustion products composition of $St_b(1250)$ in the dark flame zone with that of pure ADN at 0.6 MPa at a distance from the burning surface $L_1 \sim 4$ mm (Table 7) shows that the compositions of nitrogen-containing species and the temperatures are close. A similar conclusion was made in the investigation of ADN/HTPB(97/3) propellant⁷ and ADN/GAP(82.5/17.5) sandwiches.⁹ One can suppose that in the narrow (dark) flame zone of the propellant (~ 0.3 mm at 0.1 MPa), generally the same reactions as in the dark zone adjacent to the burning surface of pure ADN at 0.6 MPa occur. Temperature in the dark zone of propellant is higher than that of the dark zone of pure ADN by 200 K. This fact can be explained by reactions of interaction between oxidizer and binder and/or their decomposition products with formation of CO and CO₂, which occur in the CP and/or in a narrow zone near the burning surface.

Accordingly, experimental results indicate the conclusions that CuO catalyst acts in the CP. Usually the effect of additives on propellant combustion has a complicated character. Combustion chemistry of ADN-based propellants is closer to that of double-based ones than to that of the other types of propellants. In both cases reactions of nitrogen-containing species in the CP and in the gas phase play an important role. According to Ref. 23, in the case of double-based propellants a significant catalytic effect of CuO appears only when formation of a carbonaceous skeleton and the accumulation of catalyst on the burning surface take place. As this skeleton contains a large amount of agglomerates with the catalyst, the coefficient of thermal conductivity of this skeleton at the burning surface is higher than that of the propellant without additive. As a result, additional heat release appears near the burning surface. This heat release accelerates reactions in both CP and gas phase near the burning surface, and as a consequence the burning rate increases. Additionally, in the case of addition of CuO to $St_b(10,000)$ the larger increase of the burning rate in comparison with $St_b(1250)$ is caused by the larger accumulation of products of pyrolysis of

PCL(10,000) at the burning surface. However, the main mechanism of action of CuO catalyst relates to chemical reactions with it. The mentioned mechanism of increase of the burning rate caused by the accumulation of the catalyst on the burning surface and the increase of thermal conductivity of the near-surface layer is an additional one to this main mechanism.

Conclusions

Experiments on investigation of combustion of ADN/PCL propellant of stoichiometric composition at 4 MPa were conducted in conditions close to that typical of the combustion chamber of a rocket motor. It was shown that experimentally determined temperature and composition of combustion products are close to that at equilibrium. Thus, it can be stated that experimentally derived specific impulse for this propellant will be close to calculated one.

The comprehensive study of the combustion of ADN/PCL propellant showed that the burning rate of this propellant is controlled by both oxidizer and binder. Reactions of ADN decomposition are responsible for heat release in the condensed phase. On the one hand, PCL inhibits the reactions of ADN decomposition in the condensed phase. This leads to a decrease of the burning rate. On the other hand, reactions between decomposition products of PCL with those of ADN result in intensification of gas phase processes in the flame. CuO catalyst at 4 MPa increases the rate of reactions and heat release in the condensed phase and in the gas phase near the burning surface. The mechanism of influence of CuO catalyst on combustion of ADN-based propellants is probably similar to the mechanism of its influence on double-based propellants. Slight modification of the composition of the baseline propellant by minor additives of CuO or Pb₃O₄ and the use of polymers with different molecular weights allowed us to obtain a number of propellant formulations with different pressure dependence of the burning rate at 4–8 MPa.

ADN-based propellants have higher specific impulse than AP-based propellants. Also, the combustion properties of ADN-based propellants differ considerably from those of AP-based propellants making prior knowledge of AP-based propellant design of little use. This fact should be taken into account when tailoring the composition of ADN-based propellants. Data obtained via this tailoring can be used for development of a combustion model of ADN-based propellants.

Acknowledgment

This work was supported by the U.S. Army Aviation and Missile Command under the Contract DAAHO1-98-C-R151. The authors express gratitude to J. Michael Lyon, James G. Carver, and Robert L. Stanley for useful advice and discussion during performance of work.

References

- Pak, Z., "Some Ways to Higher Environmental Safety of Solid Rocket Applications," AIAA Paper 93-1755, June 1993.
- Chan, M. L., Reed, R., and Ciaramitaro, D. A., "Advances in Solid Propellant Formulations," *Solid Propellant Chemistry, Combustion, and Motor Interior Ballistics*, edited by V. Yang, T. B. Brill, and W.-Z. Ren, Progress in Astronautics and Aeronautics, Vol. 185, AIAA, Reston, VA, 2000, pp. 185–206.
- Fogelzang, A. E., Sinditskii, V. P., Egorshv, V. Y., Levshenkov, A. I., Serushkin, V. V., and Kolesov, V. I., "Combustion Behavior and Flame Structure of Ammonium Dinitramide," *Proceedings of the 28th International Annual Conference of ICT*, Fraunhofer Inst. Chemische Technologie, Karlsruhe, 1997, pp. 99-1–99-14.
- Strunin, V. A., D'yakov, A. P., and Manelis, G. B., "Combustion of Ammonium Dinitramide," *Combustion and Flame*, Vol. 117, No. 1–2, 1999, pp. 429–434.
- Korobeinichev, O. P., Kuibida, L. V., Paletsky, A. A., and Shmakov, A. G., "Molecular-Beam Mass-Spectrometry to Ammonium Dinitramide Combustion Chemistry Studies," *Journal of Propulsion and Power*, Vol. 14, No. 6, 1998, pp. 991–1000.
- Zenin, A. A., Puchkov, V. M., and Finjakov, S. V., "Physics of ADN Combustion," AIAA Paper 99-0595, Jan. 1999.
- Korobeinichev, O. P., and Paletsky, A. A., "Flame Structure of ADN/HTPB Composite Propellants," *Combustion and Flame*, Vol. 127, No. 3, 2001, pp. 2059–2065.

⁸Parr, T., and Hanson-Parr, D., "Solid Propellant Flame Chemistry and Structure," *Non-Intrusive Combustion Diagnostics*, edited by K. K. Kuo and T. P. Parr, Begell House, New York, 1994, pp. 571–599.

⁹Kuibida, L. V., Korobeinichev, O. P., Shmakov, A. G., Volkov, E. N., and Paletsky, A. A., "Mass Spectrometric Study of Combustion of GAP- and ADN-Based Propellants," *Combustion and Flame*, Vol. 126, No. 3, 2001, pp. 1655–1661.

¹⁰Weiser, V., Eisenreich, N., Baier, A., and Eckl, W., "Burning Behavior of ADN Formulations," *Propellants, Explosives, Pyrotechnics*, Vol. 24, No. 3, 1999, pp. 163–167.

¹¹Chan, M. L., Reed, R., Turner, A., Atwood, A., and Curran, P., "Properties of ADN Propellants," *Proceedings of the 5th International Symposium on Special Topics in Chemical Propulsion, Combustion of Energetic Materials*, edited by K. K. Kuo and L. T. Deluca, Begell House, New York, 2002, pp. 492–501.

¹²Ramaswamy, A. L., "Energetic-Material Combustion Experiments on Propellant Formulations Containing Prilled Ammonium Dinitramide," *Combustion, Explosion and Shock Waves*, Vol. 36, No. 1, 2000, pp. 119–124.

¹³Parr, T., and Hanson-Parr, D. M., "Solid Propellant Diffusion Flame Structure," *Proceedings of the Twenty-Sixth Symposium (International) on Combustion*, Combustion Inst., Pittsburgh, PA, 1996, pp. 1981–1987.

¹⁴Sinditskii, V. P., Fogelzang, A. E., Egorshv, V. Y., Levshenkov, A. I., Serushkin, V. V., and Kolesov, V. I., "Combustion Peculiarities of ADN and ADN-based Mixtures," *Proceedings of the 5th International Symposium on Special Topics in Chemical Propulsion, Combustion of Energetic Materials*, edited by K. K. Kuo and L. T. Deluca, Begell House, New York, 2002, pp. 502–512.

¹⁵Babuk, V. A., Vassiliev, V. A., and Naslednikov, P. A., "Experimental Study of Evolution of Condensed Combustion Products in Gas Phase of Burning Solid Rocket Propellant," *Proceedings of the 5th International Symposium on Special Topics in Chemical Propulsion, Combustion of Ener-*

getic Materials, edited by K. K. Kuo and L. T. Deluca, Begell House, New York, 2002, pp. 381–396.

¹⁶Tereshenko, A. G., Korobeinichev, O. P., Skovorodko, P. A., Paletsky, A. A., and Volkov, E. N., "Probe Method for Sampling Solid-Rocket Combustion Products at Temperatures and Pressures Typical of a Rocket Combustion Chamber," *Combustion, Explosion and Shock Waves*, Vol. 38, No. 1, 2002, pp. 81–91.

¹⁷Korobeinichev, O. P., "Flame Structure of Solid Propellants," *Solid Propellant Chemistry, Combustion, and Motor Interior Ballistics*, edited by V. Yang, T. B. Brill, and W.-Z. Ren, Progress in Astronautics and Aeronautics, Vol. 185, AIAA, Reston, VA, 2000, pp. 335–354.

¹⁸Korobeinichev, O. P., Kuibida, L. V., Paletsky, A. A., and Chernov, A. A., "Study of Solid Propellant Flame Structure by Mass-Spectrometric Sampling," *Combustion Science and Technology*, Vol. 113–114, 1996, pp. 557–572.

¹⁹Belov, G. V., ASTRA Code, Ver. 2/24, Moscow State Technical University, Moscow, 1990 (in Russian).

²⁰Fristrom, R. M., *Flame Structure and Processes*, Oxford Univ. Press, New York, 1995, pp. 100–120.

²¹Fedotova, T. D., Glotov, O. G., and Zarko, V. E., "Chemical Analysis of Aluminum as a Propellant Ingredient and Determination of Aluminum and Aluminum Nitride in Condensed Combustion Products," *Propellants, Explosives, Pyrotechnics*, Vol. 25, No. 6, 2000, pp. 325–332.

²²Zenin, A. A., "Experimental Investigation of the Burning Mechanism of Solid Propellants and Movement of Burning Products," Ph.D. Dissertation, Physical and Mathematical Sciences, Inst. of Chemical Physics, USSR Academy of Sciences, Moscow, 1976 (in Russian).

²³Denisyuk, A. P., Demidova, L. A., and Galkin, V. I., "The Primary Zone in the Combustion of Solid Propellants Containing Catalysts," *Combustion, Explosion and Shock Waves*, Vol. 31, No. 2, 1995, pp. 161–167.